

# Normal faults geometry and morphometry on Mars

D. A. Vaz (1,2), M. G. Spagnuolo (3) and S. Silvestro (4,5)

(1) Centre for Geophysics of the University of Coimbra, Observatório Astronómico da Universidade de Coimbra, Portugal, (2) CERENA - Instituto Superior Técnico, Portugal, (3) IDEAN, UBA-CONICET, Argentina, (4) Istituto Nazionale di Astrofisica (INAF), Osservatorio Astronomico di Capodimonte, Italy, (5) Carl Sagan Center, SETI Institute, USA (davidvaz@uc.pt)

## Abstract

In this report, we show how normal faults scarps geometry and degradation history can be accessed using high resolution imagery and topography. We show how the initial geometry of the faults can be inferred from faulted craters and we demonstrate how a comparative morphometric analysis of faults scarps can be used to study erosion rates through time on Mars.

## 1. Introduction

The morphology of the normal faults scarps on Mars surface are the result of two different processes: 1) faulting dynamics and 2) posterior degradation processes. Concerning the initial fault geometry, a simple geometric model with a constant dip angle of  $60^\circ$  is commonly assumed in order to estimate strain rates on Mars [e.g. 1, 2].

Despite the old age of formation, most faults scarps on Mars are generally well preserved, implying low rates of erosion after their formation. This fact has already been noted before [3], however, a comprehensive quantitative assessment has never been performed.

In this work we show how to infer the true dip angle of the faults and how to unveil the degradation history of the faults scarps, by using high resolution imagery and topography.

## 2. Datasets and methodologies

We analyze and compare the geometry of the faults as well as their present day morphometry in two distinct areas located in Phlegeton Catena and Claritas Fossae (the same areas analyzed in [4]). We use CTX stereopairs to generate DTMs (20 m/pix) and orthoimages (6 m/pix) using NASA Ames Stereo Pipeline [5]. This data is used to map and extract

automatically the heights and slope angles of the fault scarps, using the same procedure described in [6, 7]. In order to estimate the age of faulting, crater counts were performed.

We have applied a semi-automatic procedure that enables the 3D palinspastic restoration of faulted crater rims (fig. 1). Using this technique, we were able to compute slip vectors which are used to infer the geometry of the faults that deform the craters.

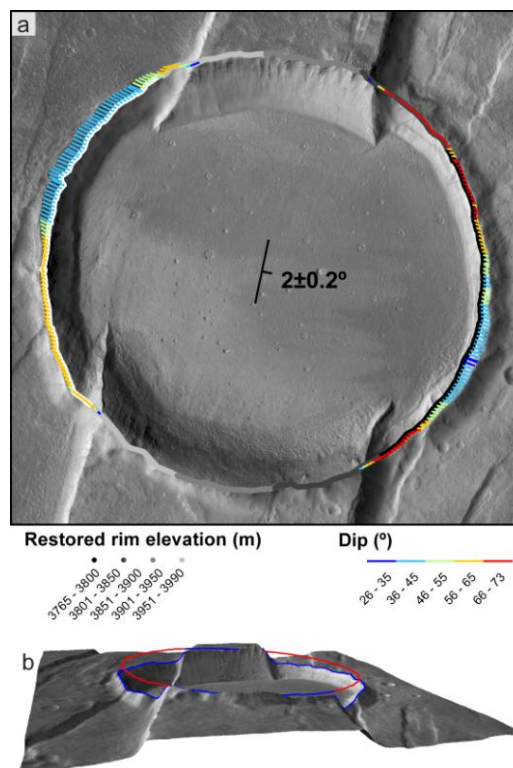


Figure 1: a) crater rim restoration vectors for the Phlegeton Catena area, the attitude of the reconstructed rim plane follows the regional topographic trend; b) 3D perspective showing the deformed (blue) and reconstructed rims (red).

A diffusive scarp degradation model is used to estimate the mass diffusivity constant [8]. This model is able to integrate the measured morphometric parameters with the ages of faulting, providing the basis for a relative morphometric dating of fault scarps on Mars.

### 3. Results and discussion

The reconstruction of the faulted rims gives different results for the two areas. In Phlegethon Catena the inferred mean dip angles were of 51.6-57.4° (fig. 1) while a lower mean angle of 46.7° was computed for Claritas. These results show that regional dip variations may exist on Mars, and that a constant angle of 60° is an approximation that may not be accurate for all regions.

We dated the faulting activity as Late Amazonian and Late Hesperian-Early Amazonian on the Phlegethon Catena and Claritas Fossae areas respectively. Combining these ages with the morphometric parameters, we were able to fit diffusive degradation models (fig. 2) which show that: 1) the faulting dip angles computed from the palinspastic reconstructions are coherent with the model results; 2) soon after the faults formation, the slopes decreased rapidly by mass wasting processes until reaching an angle  $\alpha=31-40^\circ$  (this angle corresponds to the initial talus slopes); 2) after that, diffusive processes become dominant and the slopes have been decreasing more gradually; 3) despite the different faulting ages at the two sites, the predicted diffusivities are identical ( $k\sim 4.0\times 10^{-3}$  m<sup>2</sup>/kyr). This diffusivity value represents an averaged record of the scarps degradation through time, and is three orders of magnitude below the values typically found on Earth (0.1-16 m<sup>2</sup>/kyr) [9].

### 6. Conclusions

The methods and results presented in this report, illustrate the ongoing effort we are making to better constrain the formation and evolution of normal faults scarps on Mars. The results indicate that the dip angle of normal faults is not constant and that, at least in the analyzed areas, it may be lower than the value usually assumed. Since our measurements indicate lower dip angles, this means that previous rift strain estimates on Mars were probably underestimated.

In the study areas, the low diffusivity values reported here are consistent with a hyperarid desertic environment over the last 3 Ga. The approach we use to model the scarps degradation allows the parameterization of the degradation history and enables the morphometric dating of the scarps. A more widespread survey (analyzing different areas with different faulting ages) can provide valuable information about past environmental conditions.

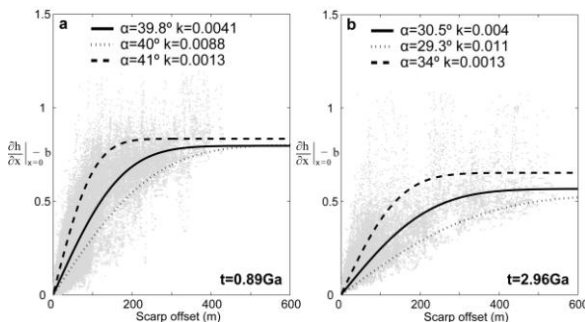


Figure 2: Best fitted degradation models for the morphometric data (scarp height vs. reduced scarp gradient,  $\alpha$  represents the initial talus slopes and  $k$  is the mass diffusivity constant) measured from the two study areas, Phlegethon Catena (a) and Claritas Fossae (b).

### References

- [1] Hauber E. and P. Kronberg (2005). *J Geophys Res-Planet*, Vol. 110 (E7).
- [2] Spagnuolo M. G., et al. (2008). *Icarus*, Vol. 198 (2),318-330.
- [3] Hauber E., et al. (2010). *Earth Planet. Sci. Lett.*, Vol. 294 (3-4),393-410.
- [4] Vaz D. A., et al. (2014) Comparative Analysis of Fault Scarps Morphometric Parameters on Mars, *45th LPSC*. No. 1777.
- [5] Moratto Z. M., et al. (2010) Ames Stereo Pipeline, NASA's Open Source Automated Stereogrammetry Software, *41st LPSC*. 2364.
- [6] Vaz D. A., et al. (2012). *Comput. Geosci.*, Vol. 48 (0),162-172.
- [7] Vaz D. A. (2011). *Planet. Space Sci.*, Vol. 59 (11-12),1210-1221.
- [8] Hanks T. C. and D. J. Andrews (1989). *J Geophys Res-Solid*, Vol. 94 (B1),565-573.
- [9] Martin Y. (2000). *Geomorphology*, Vol. 34 (1-2),1-21.